Revue des Energies Renouvelables Vol. 21 N°4 (2018) 601 - 621
DOI: https://doi.org/10.54966/jreen.v21i4.715

Performance comparison of different maximum power point trackers for photovoltaic system under fast varying of environmental conditions

Abdelhakim Belkaïd [1,2] *, Ilhami Colak [2] † and Korhan Kayisly [3] ‡

[1] Department of Electromechanics, University of Bordj Bou Arreridj
El-Anasser 34030, Bordj Bou Arreridj, Algeria
[2] Automatic Laboratory of Setif, LAS
University of Setif 1, El Maabouda, Street of Bejaia, 19000 Setif, Algeria
[3] Engineering and Architecture Faculty of Nisantasi University, Istanbul, Turkey

(reçu le 20 Décembre 2018 - accepté le 25 Décembre 2018)

Abstract - *Knowing that a large number of MPPT (maximum power point tracking) techniques exist so far and that each technique has its own advantages and disadvantages. Therefore, an appropriate examination of these techniques is indispensable to facilitate the selection of one of the more appropriate ones for a given application. This document provides a summary of these MPPT algorithms. Among them, four commonly used are examined and compared using five evaluation criteria. Perturb and observe (PO), incremental conductance (IC), sliding mode (SM), and fuzzy logic (FL) control are selected for this study and tested under a rapid change of illumination. A combined step and ramp changes in solar illumination is used to assess the effectiveness of the chosen MPPTs. The simulations of the PV system are performed by Simulink tools of MATLAB software. The results conclude that the fuzzy logic controller is the best MPP (maximum power point) tracker due to the absence of steady-state oscillations and its average efficiency of 98%. Second place belongs to the slide mode control which is the fastest and has small fluctuations. In addition, the best MPPT is successfully tested for a change in temperature and load.*

Résumé - *Sachant qu'un grand nombre de techniques MPPT existent jusqu'à présent et que chaque technique a ses avantages et ses inconvénients. Par conséquent, un examen approprié de ces techniques est indispensable pour faciliter la sélection de l'une des plus appropriées pour une application donnée. Ce document fournit un résumé de ces algorithmes MPPT. Parmi eux, quatre couramment utilisés sont examinés et comparés en utilisant cinq critères d'évaluation. Perturber et observer (PO), incrémentale de conductance (IC), mode glissant (SM), et logique floue (FL) sont sélectionnés pour cette étude et testés sous un changement rapide d'éclairement. La variation d'éclairement selon des échelons et des rampes permet d'évaluer l'efficacité des MPPT choisis. Les simulations du système PV sont effectuées par les outils Simulink du logiciel Matlab. Les résultats concluent que le contrôleur de logique floue est le meilleur suiveur MPP en raison de l'absence d'oscillations en régime permanent et de son efficacité moyenne de 98 %. La deuxième place appartient au contrôle du mode de glissement qui est le plus rapide avec de petites fluctuations. De plus, le meilleur MPPT est testé avec succès pour un changement de température et de charge.*

Keywords: Photovoltaic (PV) - Maximum power point tracking (MPPT) - Incremental conductance - Perturb and observe - Sliding mode - Fuzzy logic.

1. INTRODUCTION

Pollution of the environment has become a big problem that has worried the whole world since the beginning of the industrial revolution. So far, most of the world's electricity production comes from fossil fuels (coal, oil and natural gas) that pollute our

* belkaid08@yahoo.fr
† ilhcol@gmail.com
‡ korhankayisli@gmail.com

environment. The use of renewable sources (wind, solar, biomass, geothermal, etc.) in the production of energy (heat or electricity) is one of the solutions to reduce greenhouse gas emissions.

Photovoltaic (PV) panels can be a promising way to produce pollution free, low-cost electricity (Ameli *et al.* 2008; Farhat *et al.* 2017; Himour *et al.* 2013). Unfortunately, PV panels suffer from low conversion efficiency and their generated energy depends on environmental circumstances (Berrera *et al.* 2009). For a given couple of solar radiation and ambient temperature, PV panels have a nonlinear current versus voltage curve with only single point allowing the optimal function mode which coincides to the summit of power versus voltage characteristic.

This optimal mode can be achieved using an MPPT converter. The latter consists of a static converter controlled by a MPPT strategy. A large amount of MPPT has been proposed in several articles. Due to its simple structure and ease of implementation, the P&O algorithm is widely used in PV applications, the second most used is the IC technique (Belkaid *et al.* 2017a; Ghassami *et al.* 2013; Jubaer *et al.* 2015; Tey *et al.* 2014). Other existing MPPTs are short-circuit and open-circuit fractional techniques that use a pilot cell for measurements.

The neural network (Heidari 2016), fuzzy logic (Abdourraziq *et al.* 2016; Soufi *et al.* 2014) and sliding mode control (Belkaid *et al.* 2017b) can also be found in the literature. Each MPPT system has its own characteristics, advantages and disadvantages. Modifications are made to each technique in order to improve its performance. Comparative studies (Hohm *et al.* 2003; Esram *et al.*, 2007; Salas *et al.* 2006; Bidyadhar *et al.* 2013; Bhatnagar *et al.* 2013; Verma *et al.* 2016) between these different MPPTs are performed by many authors to facilitate selection among them for a given application.

The aim of this document is to present a comprehensive comparison and to propose which MPP tracker is most effective based on some factors including grid or off-grid application, number of stages in the power conversion chain, number of sensors required, digital or analog circuitry, dependency of PV module parameters, competence to track global MPP under partial shading situation, level of complexity, cost, efficiency and speed of tracking.

Others factors such as the instant efficiency, the average efficiency, the steady state tracking accuracy, the transient tracking accuracy and the tracking time are added to better compare four commonly used MPPTs: the perturbation and observation, the incremental conductance, the slide mode control, and fuzzy logic.

This comparative study is organized as follows; Section 2 presents the mathematical modelling of the PV panel with its static converter. The third part is dedicated to the complete description of the operating principle of each algorithm.

In section 4, the main aspects in the choice of MPP tracker are offered. The simulation results under Matlab/Simulink are presented in section 5. Finally, we come to certain conclusions.

2. MODELLING OF THE PV CONVERSION CHAIN

The main component in the considered conversion chain is the solar panel which can be modelled by an equivalent electrical circuit, consisting of an ideal current source, photocurrent I_{ph}, a diode and two resistances, in series, R_p in parallel. The PV module current I in function of the PV module voltage V is given by next formula as in (Fathy *et al.* 2017; Sahraoui *et al.* 2016):

$$I = I_{ph} - I_s\left(\exp\left(\frac{q(V + IR_s)}{N_s A k_B T}\right) - 1\right) - \frac{V + I R_s}{R_p} \tag{1}$$

Where, I_s, is the diode saturation current, N_s, number of cells related in series, A, is the diode ideality factor, q, is the electron charge (1.6 x 10^{-19} C), k_B, is Boltzmann's constant (1.38 x 10^{-23} J/K), T, is the module temperature (K).

The MSX-60 module by SOLAREX Company was utilized in this study. Its current vs. voltage characteristics and power vs. voltage characteristics under varied temperatures or under diverse irradiance levels are accessible in a lot of academic documents such as (Belkaid *et al.* 2016 a,b).

This manuscript talk about stand-alone PV panel connected to a boost topology of static converter which feeds a resistive load as shown in figure 1. The red diode is used to prevent reverse currents. The binary control signal of the switch is obtained by comparing the duty cycle of the converter with a sawtooth signal. The duty ration is determined using one of the MPPT algorithms.

The slide-based MPPT requires three sensors, but the other MPPTs need only two. The inductor L, the input capacitor C_1 and the output capacitor C_2 are used as filters. The energy extracted from the PV panel depends of two main parameters which are the solar irradiance G and the temperature T.

{Eq. (2)} gives the model of the boost configuration:

$$\begin{cases} \dfrac{di_L}{dt} = \dfrac{V - V_0}{L} + \dfrac{V_0}{L} \cdot u \\ \dfrac{dV_0}{dt} = \left(-\dfrac{V_0}{RC_2} + \dfrac{i_L}{C_2}\right) - \dfrac{i_L}{C_2} \cdot u \end{cases} \tag{2}$$

where i_L, is the current across the inductor, V_0, is the load voltage, R, is the load and u, is the position of the switch.

The technical specifications of the entire system are shown in **Table 1.**

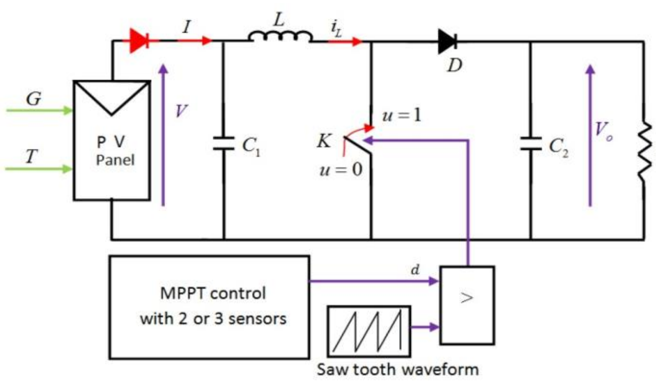

Fig. 1: The PV conversion chain

Table 1: Detailed specifications of the PV module and static converter

MSX 60 parameters	
Maximum power P_{max}	59.85 W
Open-circuit voltage V_{oc}	21.1 V

Short-circuit current I_{sc}	3.8 A
Voltage at MPPV_{mpp}	17.1 V
Current at MPPV_{mpp}	3.5 A
Temperature coefficient of V_{oc}	- 0.08 V/°C
Temperature coefficient of I_{sc}	0.003 A/°C
Boost converter parameters	
Switching frequency f	10 kHz
Inductor L	5 mH
Output capacitor C_2	47 µF
Input capacitor C_1	1000 µF
Load R	30 Ω

3. DESCRIPTION OF THE DIFFERENT MPPTS

Tracking the MPP of a PV panel is frequently a necessary part of a PV system. As such, a lot of MPPT techniques have been proposed and realized.

MPPT methods vary in complexity, required sensors, speed of convergence, cost, efficiency range, implementation material, popularity, and other considerations. In effect, so many MPPTs have been developed that it has become hard to sufficiently decide which technique, recently proposed or existing, is the most suitable for a given PV application.

In this paper, four MPPT's were chosen for comparison; PO, IC, SM and FL. Their operation principles are described below.

3.1 Perturb and observe algorithm

The perturbation and observation algorithm is the most widely used in the literature and especially in practice because of its ease of implementation. The purpose of this algorithm is to operate the system at its maximum power by incrementing or decrementing the operating point voltage and observing the effect of this perturbation on the PV output power.

According to this observation, the algorithm decides the act to be performed during the next iteration. The working principle of the PO algorithm is as described in the organizational chart of the figure 2.

At beginning, it has to detect the current and the voltage of the PV module by two sensors and then the PV power is computed as the product of them. If the disturbance causes an increase (decrease) in the power of the module, the following disturbance is performed in the same (opposite) way (Gautam *et al.* 2016).

The problem with this algorithm is: the oscillation around the MPP under constant operating conditions; the weak convergence of the algorithm in the case of sudden changes in temperature and / or illumination.

3.2 Incremental conductance algorithm

Because of its ease of implementation, the IC algorithm is the tracking strategy traditionally used. The main disadvantages compared to contemporary techniques are that in steady state, the operating point varies between neighboring values and that, under transient phenomena, it is not able to quickly follow the MPP.

Figure 3 shows the block diagram of the IC algorithm, where $k-1$ corresponds to the previous sampling instant, while k indicates the measured values in real time. The IC method follows the PV maximum power through comparison between two terms the instantaneous conductance (I/V) and the incremental conductance (dI/dV).

When the operating point reaches the maximum power, the sum of the two elements will be equal to zero. If the operating point is located in the left (right) side of the MPP, the last sum becomes greater (lower) than zero.

3.3 Slide mode control

Because of its fast dynamic response and its robustness with respect to parameter uncertainties and perturbations, SM control is very popular in the community of non-linear control systems. The working principle of SM strategy is to design a switching control law u to push the non-linear state path on a switching surface and maintain that path sliding on that surface for the entire time that follows.

The switching control signal is designed on a the base of the Lyapunov theory guarantee the movement of the stae trajectory towards a preferred behavior, knows as the sliding surface ($S = 0$) (Belkaïd *et al.* 2016b; Belkaïd *et al.* 2017b).

When the PV panel is running at its maximum power, we can make the following relationship:

$$\frac{dP}{dV} = \frac{dVI}{dV} = I + V\frac{dI}{dV} = 0 \tag{3}$$

Thus, the sliding surface is chosen as

$$S = dP / dV \tag{4}$$

And the control signal u can be defined as:

$$u = u_n + u_{eq} \tag{5}$$

The non-linear term known as the switching control takes usually the next form:

$$u_n = -k_{eq} \,.\, \mathrm{sign}(S) \tag{6}$$

where, k_{eq} is a positive constant.

In sliding mode, the dynamics of the system can be expressed by:

$$S \times \dot{S} < 0 \tag{7}$$

The second term of the switching law called equivalent control u_{eq} can be designed by means of the invariance conditions (Belkaïd *et al.* 2016b; Belkaïd *et al.* 2017b; Zhu *et al.* 2015):

$$S = 0 \quad \text{and} \quad \dot{S} = 0 \tag{8}$$

Consequently we find:

$$u_{eq} = 1 - \frac{V}{V_0} \tag{9}$$

We replace (6) and (9) in {Eq. (5)}, we can get:

$$u = 1 - \frac{V}{V_0} - k_{eq} \times \mathrm{sign}\left(\frac{dP}{dV}\right) \tag{10}$$

3.4 Fuzzy logic control

Fuzzy logic is a nonlinear controller, can work with inaccurate inputs without the need for a precise mathematical model. On the other hand, the designer must have more knowledge about the operation of PV panels. Three main steps are necessary when designing the Fuzzy Logic control, as shown in figure 4: fuzzification, inference engine and defuzzification (Ali *et al.* 2014).

First, the physical variables are rehabilitated into linguistic variables. After that, the inference method by means of If-Then rules establishes the fuzzy output in function of the inputs. Generally in literature we find the method of inference of Mamdani and that of Sugeno.

In this document, Fuzzy inference is performed using the Mamdani method. In the third step, defuzzification uses the center of gravity strategy to calculate the duty cycle that is the output of this control system as given by the following expression (Choudhury *et al.* 2015; Menadi 2015):

$$dD_0 = \frac{\sum_{j=1}^{n} \mu(D_j) - D_j}{\sum_{j=1}^{n} \mu(D_j)} \tag{11}$$

The fuzzy inputs employed here are the error E and the change of error ΔE as in (Soufi et al. 2014).

$$E(k) = \frac{P(k) - P(k-1)}{V(k) - V(k-1)} \tag{12}$$

$$\Delta E(k) = E(k) - E(k-1) \tag{13}$$

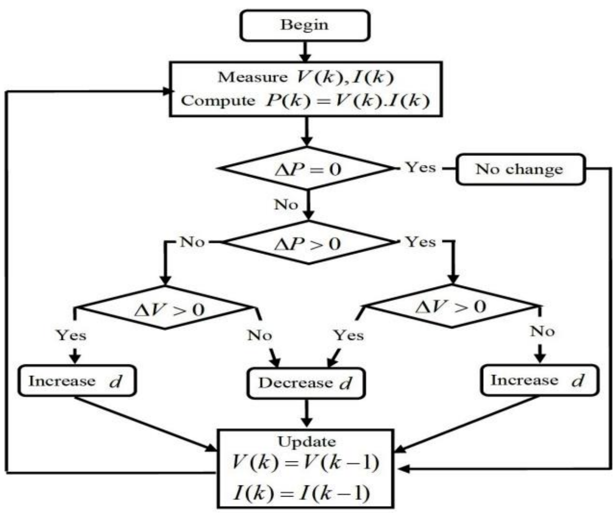

Fig. 2: Algorithm scheme (Belkaïd *et al.* 2017a)

Table 2: Fuzzy rules table

ΔE / E	NB	NS	ZE	PS	PB
NB	ZE	ZE	PB	PB	PB
NS	ZE	ZE	PS	PS	PS
ZE	PS	ZE	ZE	ZE	NS
PS	NS	NS	NS	ZE	ZE
PB	NB	NB	NB	ZE	ZE

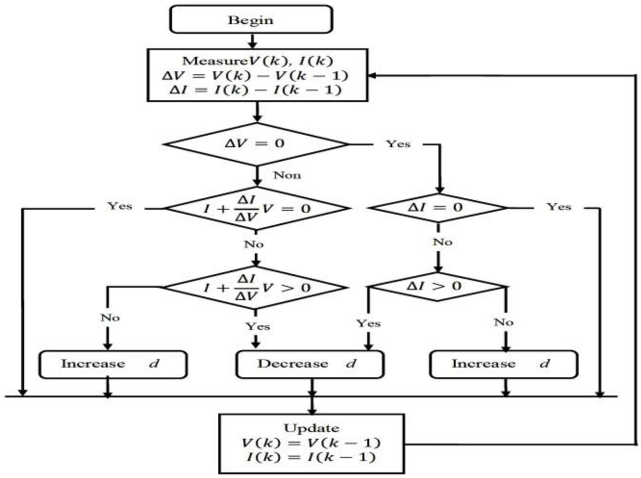

Fig. 3: IC algorithm scheme (Belkaïd *et al.* 2016a)

The FL-MPPT block provides the duty ratio of the converter. When the fuzzy entries are computed, they are converted into linguistic variables based on a membership function (MF). Each of these entries is expressed by five MFs: Big Negative (BN), Negative (N), Zero (Z), Positive (P), Big Positive (BP). The various associations between the error E and the change or ΔE give 25 responses for the boost duty cycle, as shown in **Table 2**.

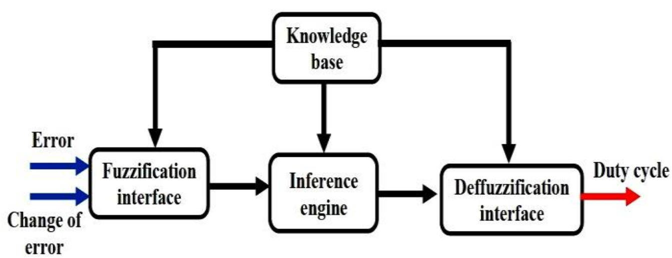

Fig. 4: Structure of FL controller

References (Aït Cheikh *et al.* 2007; Bouchafaa *et al.* 2010) presented a comparison between an intelligent method based on fuzzy logic (FL) and that of perturb and observe (P&O). They show that FL displays better performance, has a faster response time in dynamics, and a smoother power signal around steady-state maximum power. The major flaw of MPPT based on FL control when used alone is its inability to handle partial shading.

3.5 Fractional open circuit voltage technique (FOCV)

The fractional open circuit voltage technique is based on the fact that the output voltage at the MPP of the PV panel depends linearly on its open circuit voltage for different levels of illumination and temperature, i.e.:

$$V_{mpp} \approx k_{oc} \times V_{oc} \tag{14}$$

Where k_{oc} is a proportionality constant which is limited between 0.72 and 0.78 (Verma *et al.* 2016). V_{oc} must be measured at each period by briefly opening the circuit, this causes the temporary loss of energy. To avoid this drawback, we use pilot cells from which we can obtain V_{oc}

These pilot cells must have characteristics identical to those of the photovoltaic panel used. After, V_{mpp} is calculated using (14) which is only an approximation, it means that the panel never reaches the true MPP. According to the PV system application, this method can occasionally be suitable. The FOCV technique is very simple and inexpensive to implement because it does not really need a DSP or a microcontroller.

3.6 Fractional short circuit current technique (FSCC)

The fractional short circuit current technique is based on the fact that the output current at the MPP of the PV panel is quasi linear proportional on its short circuit current under change of environment conditions, i.e.:

$$I_{mpp} \approx k_{sc} \times I_{sc} \tag{15}$$

Where k_{sc}, is a proportionality factor which is bounded between 0.78 and 0.92 (Verma *et al.*). The constant k_{sc} as k_{oc} depends on the PV panel used.

To measure the I_{sc} the PV panel must be short-circuited periodically with an interrupter added to the static converter that increases the number of components and also the total cost of the system. By using a boost converter we can avoid the additional switch.

On the other hand, the accuracy of these techniques is low, in particular because of the methods for estimating the characteristic parameters of the PV panel (I_{sc} and V_{oc}). In addition, whenever a measurement of current or voltage is made, this entails a mandatory power transfer stop and therefore energy losses that are not negligible.

3.7 Artificial neural networks (ANN)

ANN is among the smart commands, it is based on the electronic neuronal arrangement of the brain. Neural networks associate the inputs to the outputs via via a hidden layer as depicted in figure 5.

The diagram of this last figure shows that solar irradiance and temperature are used as two input neurons, the output neuron is represented by the duty cycle of the power converter, the hidden layer is constructed by five neurons. The neuron in the hidden layer receives data from the input layer, calculates their outputs using the sigmoidal activation function, and then transmits them to the output layer.

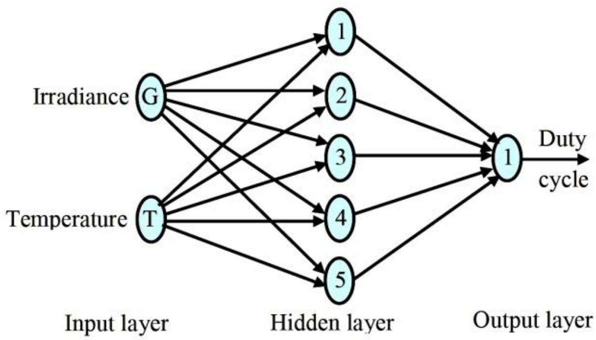

Fig. 5: Structure of neural network controller

3.8 Particle Swarm Optimization (PSO)

The PSO is a soft computing algorithm based on the analysis of the similarity of social behaviour and movements of animals such as birds and schools of fish. The PSO method can be useful for any optimization difficulty that has a multivariate function with several optimal points (Bidyadhar *et al.* 2013).

The PSO is very efficient to follow the global MPP in case of partial shading condition where more than one maximum point exists. The displacement of the PSO (swarm) agent into the search space depends on its own better anterior position and the best overall position for all swarms. For each position, the power calculation is performed for all agents, thereby MPP reached.

3.9 Temperature based technique (T-MPPT)

Temperature is the second most important parameter in the behavior of the solar cell. The theoretical characteristics $I-V$ and $P-V$ of the solar cell under a constant illumination and under different temperatures show that the short-circuit current remains very little sensitive to the variation of the temperature but the open circuit voltage decreases by increasing the temperature which causes a decreased power at the exit of the solar cell. The open circuit voltage as a function of temperature is given by (Tafticht *et al.* 2008):

$$V_{oc} = V_{oc}^{*} + \delta \,.\, (T - T^{*}) - r_s \,.\, (I_{sc} - I_{sc}^{*}) \qquad (16)$$

where r_s , is a series resistance and δ, is a coefficient obtained empirically ($V / °C$).

According to temperature change the voltage at $MPP\ V_{mpp}$ varies approximately as V_{oc}. The temperature based MPPT was born from the fact that the output voltage is directly proportional to the temperature on the panel surface, as described in (17):

$$V_{mpp}(T) = V_{mpp}(T^{*}) + k_{mpp} \,.\, (T - T^{*}) \qquad (17)$$

where $V_{mpp}(T)$ is an optimal voltage for a given temperature T; $V_{mpp}(T^{*})$ is an optimal voltage for a reference temperature T^{*}; k_{mpp} is a temperature coefficient of V_{mpp}. The parameters k_{mpp} and V_{mpp} at T^{*} are given in the PV module datasheet.

Most MPPT techniques use two sensors to measure current and voltage. But in the technique based on the measurement of the temperature, the current sensor is replaced by a temperature sensor, fixed on the rear face of the panel.

3.10 Ripple correlation control (RCC)

This algorithm in its pursuit of maximum power uses ripples of the power signal caused naturally by the opening and closing of the switch of the static converter which serves as an interface in the PV conversion system. RCC correlates the dp / dt with the di / dt or dv / dt to bring the power gradient to zero, thus achieving the MPP.

If v or i increases and p increases too, then the operating point is located under the MPP. On the other hand, if V or I increases and P decreases, then the operating point is overhead the MPP. Joining these two observations, we can see that the products $dP / dt \ x \cdot dV / dt$ or $dP / dt \ x \cdot dI / dt$ are positive in the left side of the MPP, negative to the right side of the MPP, and zero at the MPP.

In the case where the employed static converter is of type of boost topology, the increase in the duty cycle increases the current of the PV panel, but decreases the voltage of the latter. Therefore, the duty cycle d can be expressed by (18) or (19) as in (Bidyadhar *et al.* 2013):

$$d = -k_d \times \int \frac{dP}{dt} \times \frac{dV}{dt}\, dt \tag{18}$$

$$d = k_d \times \int \frac{dP}{dt} \times \frac{dI}{dt}\, dt \tag{19}$$

where k_d is a constant.

3.11 Look-up table method (LT)

Databases rich in current and voltage measurements for different environmental conditions of illumination and temperature are needed for this method in order to follow the MPP.

MPPT based on look-up tables of module characteristics, should be able to instantly determine the optimum operating point when solar radiation and/or temperature readings are available; however, the non-linearity and the change of solar module characteristics according to these variables make it difficult to establish and store a reliable look-up table.

This technique has a slow convergence speed, needs a great data storage and fails in case of fast changing in climatic conditions; Similarly, it cannot follow the global MPP in case of partial shading situation.

3.12 Curve fitting technique (CF)

The power-voltage characteristic of the PV module is nonlinear and can be modelled mathematically using a curve fitting method. This characteristic can be estimated as a cubic polynomial equation:

$$P = aV^3 + bV^2 + cV + d \tag{20}$$

The derivative dP/dV is zero at the MPP

$$\frac{dP}{dV} = 3a\,V^2 + 2b\,V^1 + c = 0 \tag{21}$$

The coefficients a, b, c and d can be determined by sampling k values of PV voltage, current, and power. Afterwards, the optimal voltage that is the solution of (21) can be calculated and the MPP will be located.

$$V_{mpp} = \frac{-b \pm \sqrt{b^2 - 3ad}}{3a} \tag{22}$$

A modified curve fitting method that expresses the PV power as a function of the temperature and voltage of the panel in fourth-order polynomial form has been provided by (Leedy *et al.* 2013).

$$P = eT\,V^4 + f\,T\,V^3 + g\,V^2 + hT\,V + iT \tag{23}$$

with e, f, g, h and i are coefficients.

3.13 Three point technique (TP)

As its name implies, the three-point method compares the power of three points (the power at the current point P_n, that of the previous point P_{n-1} and that of the next point (P_{n+1}) of the solar panel $P-V$ characteristic. If the power P_{n+1} is greater than or equal to the power P_n, a positive perturbation is assigned otherwise a negative disturbance. If the power P_{n-1} is smaller than P_n, a positive disturbance is applied, otherwise a negative disturbance as indicated in **Table 3**.

The three power points are compared after each disturbance of the voltage and the duty cycle of the converter is modified consequently. The main advantage of this type of $MPPT$ is the no oscillation around MPP (Jiang *et al.* 2005; Hohm *et al.*, 2003).

Table 3: Three point $MPPT$ (Bhatnagar *et al.* 2013)

State	Control action
$P_{n+1} > P_n$ & $P_{n-1} > P_n$	No change
$P_{n+1} > P_n$ & $P_{n-1} < P_n$	Increase d
$P_{n+1} > P_n$ & $P_{n-1} = P_n$	No change
$P_{n+1} < P_n$ & $P_{n-1} > P_n$	Decrease d
$P_{n+1} < P_n$ & $P_{n-1} < P_n$	No change
$P_{n+1} < P_n$ & $P_{n-1} = P_n$	Decrease d
$P_{n+1} = P_n$ & $P_{n-1} > P_n$	No change
$P_{n+1} = P_n$ & $P_{n-1} < P_n$	No change
$P_{n+1} = P_n$ & $P_{n-1} = P_n$	No change

4. MAIN ASPECTS IN THE CHOICE OF MPPT METHOD

4.1 Number of sensors

According to the theory above, the different $MPPT$ techniques can be classified according to the number of parameters to be controlled, or in other words depending on the number of sensors required to measure the input variables of the $MPPT$ command.

So, $MPPT$ techniques can be classified into two types, such as one-sensor and two-sensor techniques. The variables that can be sensed for an $MPPT$ block are voltage, current, temperature, sunshine or can be a combination of them. It should be noted that it is easier and less expensive to use a voltage sensor while the current sensor is expensive and bulky and, therefore, the use of the current sensor is troublesome in PV systems.

It might be better to use $MPPT$ schemes that only need one sensor as in (Kasa *et al.* 2005), the PV current is estimated from the PV voltage, eliminating the necessity for a current sensor.

4.2 Digital or analog implementation

Another aspect to consider in selecting which $MPPT$ is appropriate for a given application is the need for analog, digital, or both circuits to implement it. However, it depends a lot on the knowledge of the users.

Some users are more familiar with analog circuits; in this case FSCC or FOCV, and RCC are more preferred. Others are more familiar with digital circuits, although this may require the use of software and programs; in this case, P&O, IC, FL control and the neural network are right alternatives.

4.3 Monetary costs

The use of MPPT commands in photovoltaic panels is intended to reduce the cost of the energy they generate. This aspect indicates which MPPT technique is more economical compared to others.

The method used to estimate the cost of any tracking strategy is directly linked to the number of sensors required, the computation procedure and the circuits employed to implement them.

Methods requiring complex circuits are more expensive. It is not easy to provide the exact cost of each MPP tracker because of the lack of cost data by the designer.

4.4 Applications

MPPT techniques can be classified according to the type of installation on which they can be applied. There are two types of system, stand-alone system and network-connected system.

4.5 Stages of power conversion

Generally a PV conversion chain is constructed by one or two stages. A stage is only a static converter which can be either DC-DC type or DC-AC type. A MPPT technique can be applied to t he DC-DC converter, the DC-AC converter, or both.

4.6 PV parameters dependence

Some MPPTs are dependent and others are independent of PV parameters. For example, FOCV method and FSCC method are respectively dependent on V_{co} and I_{sc}.

4.7 Competence for partial shading

The appearance of several local maxima on the $P-V$ characteristic due to the partial shading of the PV panel located next to trees or buildings can be a real obstacle to the proper functioning of a MPPT controller.

A considerable loss of power can be observed if a local maximum is followed instead of the global maximum (true MPP). Some existing MPPT methods such as ANN, FL control and PSO based method are efficient to track the true MPP under partial shading situation. Others like P&O and IC techniques are not competent to defeat the problem of partial shading.

4.8 Efficiency of tracking

This factor measures the efficiency of the MPPT command and gives the percentage of the system operating point position relative to the PPM. According to this aspect, the different MPPTs can be classified in four categories: low, medium, high and very high.

4.9 Speed of tracking

A MPPT command must have a good behaviour in dynamics in order to be able to ensure that the search for the new MPP, as a result of changes in luminosity or temperature, is made as quickly as possible.

Table 4 provides a brief comparison of different MPPTs and shows that all methods have their own pros and cons. The table is supposed to serve as a helpful guide in choosing the correct MPPT technique for specific PV applications.

Table 4: Comparison of different MPPTs according to various aspects

Stages of power conversion=SPC, PV parameters dependence=PD, Competence for partial shading=CPS

MPPT	Application	SPC	Sensors	PD	Simplicity	Tracking efficiency	Tracking speed	Analog or digital	Monetary cost	CPS
P&O	autonomous	both	V & I	no	Simple	medium	slow	A & D	medium	no
IC	autonomous	both	V & I	no	Medium	high	medium	D	medium	no
FOCV	autonomous	dc-dc	V	yes	Simple	low	fast	A & D	inexpensive	no
FSCC	autonomous	dc-dc	I	yes	Simple	low	fast	A & D	inexpensive	no
SM	both	both	V or I	no	Medium	high	fast	D	expensive	yes
FL	both	dc-dc	V & I	yes	Complex	very high	fast	D	expensive	yes
ANN	grid	dc-dc	V & I	no	Complex	very high	fast	A & D	expensive	yes
PSO	autonomous	both	V & I	no	Medium	high	fast	A & D	expensive	yes
T-MPPT	autonomous	dc-dc	V & I	yes	Simple	high	fast	D	expensive	no
RCC	both	dc-ac	V or I	yes	Complex	high	slow	A	expensive	no
LT	autonomous	dc-dc	V & I	yes	Simple	medium	fast	D	inexpensive	no
CF	autonomous	dc-dc	V	yes	Simple	medium	fast	D	inexpensive	no
TP	autonomous	both	V & I	no	Complex	high	slow	A & D	expensive	no

5. ANALYSIS OF SIMULATION RESULTS AND COMPARISON

The system discussed in this document is shown in figure 1 and its detailed specifications are given in **Table 1**. It consists of a boost chopper used as an interface between the source of the solar panel and a resistive load. The diverse chosen MPPT algorithms are implemented into Matlab/Simulink environment and tested with same parameters of irradiance, temperature and load, in order to show how they are performing against each other.

Consequently, to acquire this object, a rigorous profile composed by varied shapes as recommended by the European Norm EN 50530 has been used for the solar radiation as exposed in figure 6. All simulations are done using the atmospheric temperature of 25 °C and constant resistance of 30 Ω. However, the irradiance takes many forms such as step-down, step-up, ramp-down and ramp-up.

The object of this comparative work is to suggest which method amongst others is the more efficient on the base of multi-criteria:

-The tracking accuracy or the instant efficiency T_{acc} (Bizon 2016; Jubaer et al. 2015):

$$T_{acc} = \frac{P_{MPPT}}{P_{max}} \times 100 \quad (\%) \tag{24}$$

Where P_{MPPT} is the reached power using a given MPPT method and P_{max} is the theoretical maximum power.

-The tracking or the average efficiency T_{eff} can be estimated as follows (Bizon 2016; Jubaer et al. 2015; Sarigiannidis *et al*. 2015)

$$T_{eff} = \frac{\int_0^t P_{MPPT}}{\int_0^t P_{max}} \times 100 \quad (\%) \tag{25}$$

-The tracking time t_r which can be described as the required time to get the new MPP when the illumination changes.

-The steady-state tracking ac.

-Accuracy T_{s_acc} determines the performance of the $MPPT$ system in stationary state, i.e. how the algorithm moves toward the actual MPP under fixed irradiance.

-The transient tracking accuracy T_{t_acc} computes the $MPPT$ performance in a dynamic situation, i.e. how the $MPPT$ technique acts in response to sunlight changes.

Figure 7 shows the simulation results for abrupt change in solar radiation with the four chosen control schemes, where the power waveform of the tracked MPP achieved by a particular MPPT is compared to that obtained by the others and to the theoretical peak power point P_{max}.

Enlarged images were taken at different locations to better distinguish the difference between the maximum power behaviours tracked by the selected extracting techniques in transient and stationary situations. The zooms added to figure 7 indicate from left to right respectively: the steady-state performance, the step-down transient, the step-up transient, and the ramp-down transient.

It can clearly be seen that all the methods miss their tracking trajectory if the variation of the irradiance is in the form of a ramp with the exception of the FL tracker which does not lose its direction of tracking during the descents of the irradiance. Another remark is that the SM controller has the best response time compared to other MPPTs when sunlight changes suddenly.

However, under such conditions, FL needs more time to obtain MPP. Although all techniques exhibit power oscillation during the transient period, this behavior can not significantly affect the total efficiency of the PV system. In zoom of the stable state, one can observe that the true MPP is equal to 59.75 W for irradiance of 1000 W/m^2, the MPP followed by the FL control is without oscillations and very close to the theoretical value, the SM tracks the maximum power with a very low ripple, the PO algorithm takes the third place with an average ripple amplitude and finally IC method generates maximum power with a large ripple of 3 watts.

The major benefit of FL is the non existence of steady-state MPP oscillations, which makes energy loss almost nil. The instantaneous behaviour of the tracking capability for each method discussed under a rapid change of solar radiation is depicted in Fig. 8 in which a comparison between their average efficiency is shown.

The largest value of the power transfer efficiency is obtained for the FL controller, its average value is equal to ($T_{eff-FL} = 97.95\%$), the second place comes to basic SM tracker with average efficiency of ($T_{eff-SM} = 97.73\%$), followed by ($T_{eff-PO} = 97.58\%$) for the PO algorithm and then by ($T_{eff-IC} = 97.28\%$) for IC technique. Moreover, one can observe that the FL and SM techniques have an instantaneous tracking efficiency greater than 99 % at any time, with the exception of transient periods where the curve has profound descents.

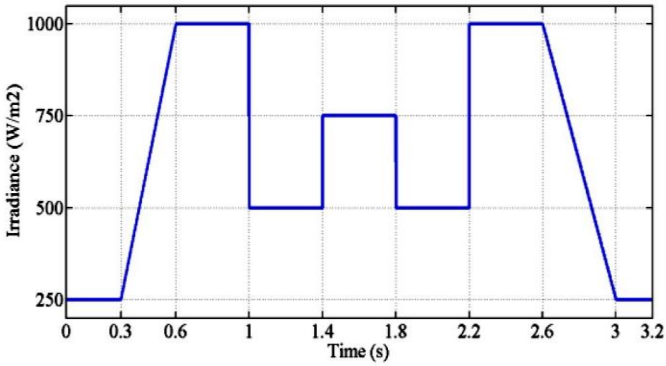

Fig. 6. Illumination change

To give more details on this comparison, numerical results of the simulation are summarized in two tables. Table 5 compares the considered MPPTs by three criteria of evaluation as: the follow-up time, tracking accuracy, and tracking efficiency. **Table 6** compares the same techniques by means of the transient and steady-state tracking efficiency.

After this in-depth analysis, we can conclude that the fuzzy logic controller is the best MPP tracker according to: its overall average efficiency of about 98%, its instantaneous tracking capability greater than 99 %, no steady-state MPP oscillations, and the acceptable tracking speed. Second place belongs to the nonlinear slide mode control which is the fastest and has small fluctuations.

The resulting curves of the best MPP follower are shown in figure 9. The PV current, PV power, and PV voltage are provided in association with the output voltage of the converter. From these curves, it can be confirmed that the different quantities have reached values similar to those given by the MSX 60 characteristics (Belkaïd *et al.* 2016a). In addition, the current and power waveforms are significantly affected by the change of illumination, whereas the voltage is only slightly affected.

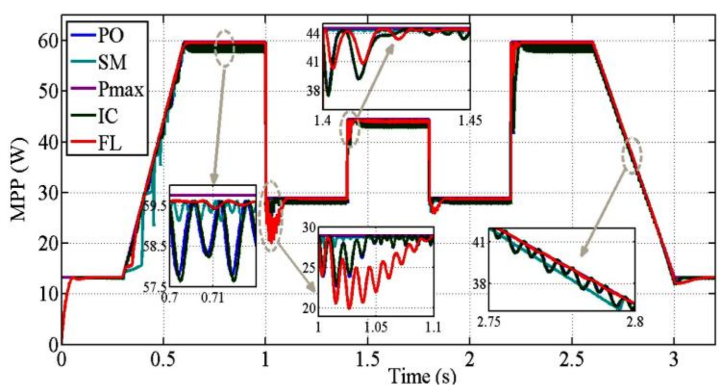

Fig. 7: Power response to fast change in irradiance for the selected MPPTs

Moreover, by comparing the PV voltage to the load voltage, it can be confirmed that the power converter used is of the boost type. Under standard test conditions ($G = 1000\,W/m^2$, $T = 25°C$), the PV module generates a maximum power of approximately 60 W corresponding to an optimum voltage of 17.1 V and an optimum current of 3.5 A. The behavior of the boost duty cycle corresponding to the used irradiance profile is illustrated in figure 10.

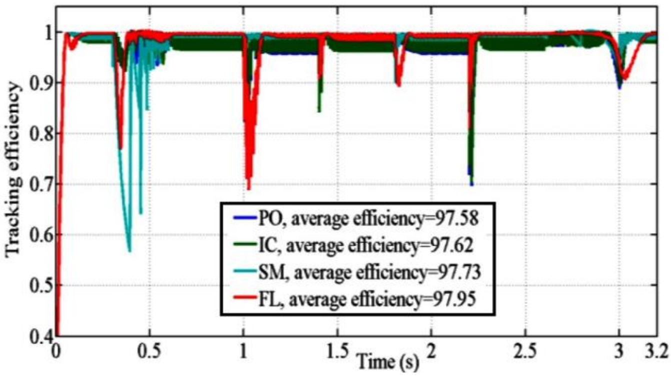

Fig. 8: Performance comparison by tracking efficiency

Table 5: Performance evaluation using: the follow-up time, tracking accuracy, and tracking efficiency

Method	t_r (s) Start-up	t_r (s) Step-up	t_r (s) Step-down	T_{acc} (%) Min	T_{acc} (%) max	T_{eff} (%)
IC	0.05	0.013	0.0001	65.90	100.30	97.28
PO	0.05	0.017	0.0001	69.81	100.31	97.58
SM	0.05	0.0001	0.008	56.71	100.30	97.73
FL	0.05	0.016	0.05	69.00	100.30	97.95

Table 6: Performance evaluation using: the transient and steady-state tracking efficiency

G (W/m^2)	250	500	750	1000	250 → 500	500 → 1000
IC	$T_{s\_acc}=98.11$	$T_{s\_acc}=97.31$	$T_{s\_acc}=96.87$	$T_{s\_acc}=96.5$	$T_{t\_acc}=96.59$	$T_{t\_acc}=97.11$
PO	$T_{s\_acc}=98.52$	$T_{s\_acc}=97.59$	$T_{s\_acc}=97.24$	$T_{s\_acc}=96.95$	$T_{t\_acc}=97.91$	$T_{t\_acc}=97.58$
SM	$T_{s\_acc}=98.61$	$T_{s\_acc}=99.08$	$T_{s\_acc}=99.27$	$T_{s\_acc}=99.33$	$T_{t\_acc}=98.70$	$T_{t\_acc}=99.11$
FL	$T_{s\_acc}=98.95$	$T_{s\_acc}=98.96$	$T_{s\_acc}=98.78$	$T_{s\_acc}=99.38$	$T_{t\_acc}=98.77$	$T_{t\_acc}=99.08$

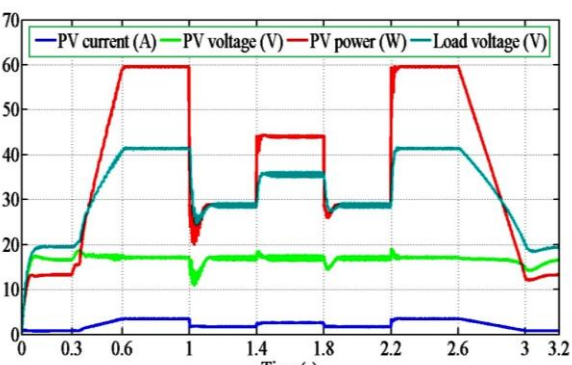

Fig. 9: Resulting curves obtained by the FL technique during a rigorous irradiance signal

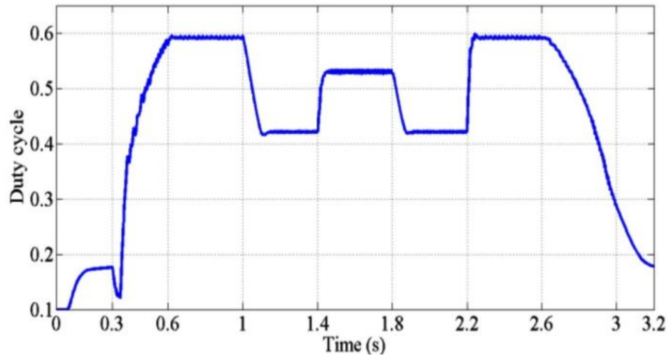

Fig. 10: Duty cycle behaviour when the converter is controlled by the fuzzy method during a rigorous irradiance signal

A second factor that affects photovoltaic conversion after sunlight is temperature, so we test with this factor the most efficient MPPT technique.

A temperature change profile is chosen in the trapezoidal form evolving from 0 °C to 50 °C as that of figure 11**a**, the irradiation is kept constant at $G = 1000\,W/m^2$ and the resistance is set at 30 Ω. The results obtained are illustrated in figure 11**b**. It can be seen that the waveforms of PV voltage, PV power are inversely proportional to the temperature change and the PV current is only slightly affected.

The last test concerns the change of load as shown in figure 12**a**. The corresponding results are shown in figure 12**b**. They show that PV quantities, power, voltage and current are not affected by the change in resistance.

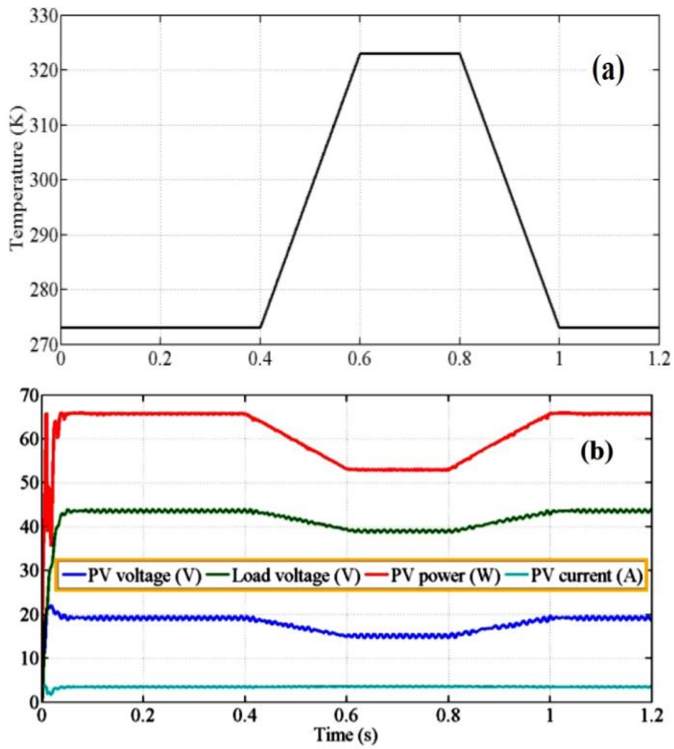

Fig. 11: (**a**) Temperature change, and (**b**) corresponding results

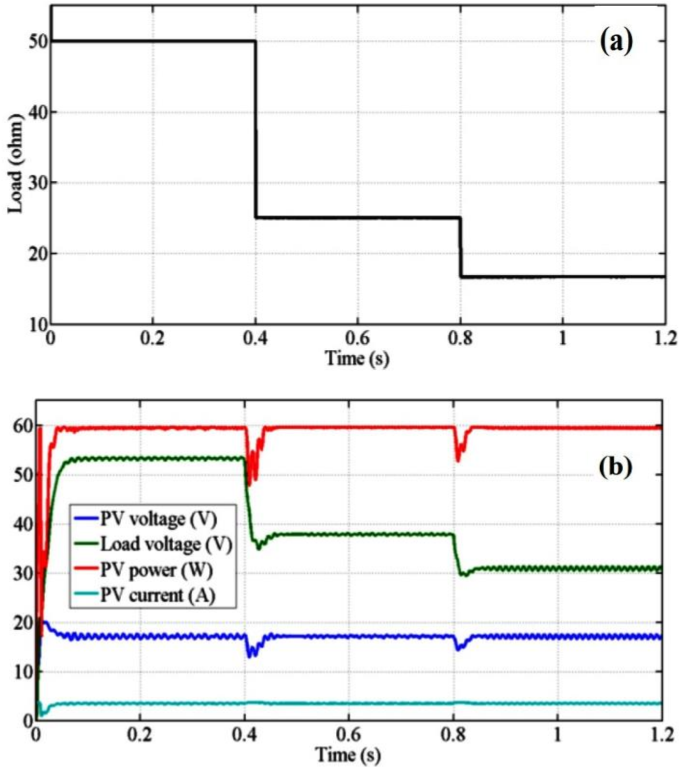

Fig. 12: (**a**) Load change, and (**b**) corresponding results

6. CONCLUSIONS

This document presents a synthesis of several MPPTs and their classification on the basis of 09 evaluation criteria. The comparative analysis provided here may prove to be a good tool that can guide the selection of the most appropriate MPPT type for a particular application.

An extended comparison of the four most widely used MPPT methods in PV systems was also provided. Many evaluation criteria counting: grid or off-grid application, stages of power conversion, sensors required, digital or analog circuitry, dependency of PV parameters, competence to track global MPP under partial shading situation, level of complexity, cost, efficiency and speed of tracking are considered.

According to steady-state MPP oscillations, the studied methods can be classified from the best to the worst as follows: FL , SM , IC and finally PO.

Based on the dynamic performance, the considered MPPTs can be organized from the highest to the lowest tracking speed in the following order: SM , IC, PO and FL . However, the tracking speed is less important than the yield of the generated power.

The results demonstrate that the FL algorithm performs significantly better than the other algorithms, offering precise tracking under rapidly changing irradiation, temperature, and load conditions.

Acknowledgments- This research work has been supported by the CNEPRU project N° **A01L07UN340120150001**, conducted at the Electromechanical Department, Faculty of Science and Technology, Bordj Bou Arreridj University, Algeria. It has also been supported in part by the Engineering and Architecture Faculty of **Nisantasi University**, Istanbul, Turkey. This support is gratefully acknowledged.

REFERENCES

[1] M. Abdourraziq, M. Ouassaid and M. Maaroufi, '*Single-Sensor Based MPPT for Photovoltaic Systems*', International Journal of Renewable Energy Research, Vol. 6, N°2, pp. 570 - 576, 2016.

[2] M. Aït Cheikh, C. Larbes, G. Tchoketch Kebir and A. Zerguerras, '*Maximum power point tracking using a fuzzy logic control scheme*', Revue des Energies Renouvelables, Vol. 10, N°3, pp. 387 – 395, 2007.

[3] A. Ali, A. Hasan and T. Marwala, '*Perturb and Observe Based on Fuzzy Logic Controller Maximum Power Point Tracking (MPPT)*', 3rd International Conference on Renewable Energy Research and Applications (ICRERA), Milwakuee, USA 19-22 Oct 2014, pp. 406 - 411, 2014.

[4] M. Ameli, S. Moslehpour and M. Shamlo, '*Economical load distribution in power networks that include hybrid solar power plants*', Electric Power Systems Research, Vol. 78, N°7, pp. 1147 - 1152, 2008.

[5] A. Belkaid, I. Colak and O. Isik, '*Photovoltaic maximum power point tracking under fast varying of solar radiation*', Applied Energy, Vol. 179, pp. 523 - 530, 2016a; http://dx.doi.org/10.1016/j.apenergy.2016.07.034 .

[6] A. Belkaid, I. Colak and K. Kayisli, '*Implementation of a modified P&O-MPPT algorithm adapted for varying solar radiation conditions*', Electrical Engineering - Springer. Vol. 99, N°3, pp. 839 - 846, 2017. Doi 10.1007/s00202-016-0457-3.

[7] A. Belkaid, J.P. Gaubert and A. Gherbi, '*An improved sliding mode control for maximum power point tracking in photovoltaic systems*', Journal of Control Engineering and Applied Informatics, Vol. 18, N°1, pp. 86 - 94, 2016.

[8] A. Belkaid, J.P. Gaubert and A. Gherbi, '*Design and implementation of a high performance technique for tracking photovoltaic peak power*', IET Renewable Power Generation. Vol. 11, N°1, pp. 92 - 99, 2017b. Doi: 10.1049/iet-rpg.2016.0023.

[9] M. Berrera, A. Dolara, R. Faranda and S. Leva, '*Experimental test of seven widely adopted MPPT algorithms*', IEEE Bucharest Power Tech Conference, June 28th – July 2nd, Bucharest, Romania, 2009. Doi: 10.1109/PTC.2009.5282010.

[10] P. Bhatnagar and R.K. Nema, '*Maximum power point tracking control techniques: state-of-the-art in photovoltaic applications*', Renewable and Sustainable Energy Review, Vol. 23, C, pp. 224 - 241, 2013.

[11] S. Bidyadhar and R.A. Pradhan, '*Comparative study on maximum power point tracking techniques for photovoltaic power systems*', IEEE Transactions on Sustainable Energy, Vol. 4, N°1, pp. 89 - 98, 2013.

[12] F. Bouchafaa, D. Beriber and M. Boucherit, '*Modeling and Simulation of A Gird Connected PV Generation System With MPPT Fuzzy Logic Control*', 7th International Multi-Conference on Systems, Signals and Devices. 2010.

[13] N. Bizon, '*Global Extremum Seeking Control of the power generated by a Photovoltaic Array under Partially Shaded Conditions*', Energy Conversion and Management, Vol. 109, pp. 71 - 85, 2016.

[14] S. Choudhury, P. Kumar Rout, '*Adaptive Fuzzy Logic based MPPT Control for PV System Under Partial Shading Condition*', International Journal of Renewable Energy Research, Vol. 5, N°4, pp. 375 - 383, 2015.

[15] T. Esram and P.L. Chapman, '*Comparison of photovoltaic array maximum power point tracking techniques*', IEEE Transactions on Energy Conversion, Vol. 22, N°, pp. 439 – 449, 2007.

[16] M. Farhat, B. Oscar, L. Sbita et al. '*A robust MPP tracker based on sliding mode control for a photovoltaic based pumping system*'. International Journal of Automation and Computing Archive, Vol. 14, N°4, pp. 489 - 500, 2017. https://doi.org/10.1007/s11633-016-0982-6

[17] A. Fathy, I. Ziedan and D. Amer, '*Improved teaching–learning-based optimization algorithm-based maximum power point trackers for photovoltaic system*', Electric Engineering, Springer, 2017. https://doi.org/10.1007/s00202-017-0654-8.

[18] S. Gautam, D. Raut, P. Neupane, D. Ghale and R. Dhakale, '*Maximum Power Point Tracker with solar prioritizer in Photovoltaic application*', 5th International Conference on Renewable Energy Research and Applications (ICRERA), Birmingham, UK, 20-23 Nov 2016, 1051-1054, 2016.

[19] A. Ghassami, S. Sadeghzadeh and A. Soleimani, '*A high performance maximum power point tracker for PV Systems*', Electric Power Energy System, Vol. 53, pp. 237 - 243, 2013.

[20] M. Heidari, '*Improving Efficiency of Photovoltaic System by Using Neural Network MPPT and Predictive Control of Converter*', International Journal of Renewable Energy Research, Vol. 6, N°4, pp. 1524 - 1529, 2016.

[21] K. Himour, K. Ghedamsi and E. Berkouk, '*Modeling and Control of a Three Level DCI in a Grid Connection Photovoltaic/Battery Storage System*', International Journal of Renewable Energy Research, Vol. 3, N°3, pp. 488 - 497, 2013.

[22] D.P. Hohm and M.E. Ropp, '*Comparative study of maximum power point tracking algorithms*', Progress in Photovoltaics: Research and Applications Vol. 11, N°1, pp. 47 - 62, 2003. http://dx.doi.org/10.1002/pip.459.

[23] Jiang Joe-Air, Huang Tsong-Liang, Hsiao Ying-Tung, Chen Chia-Hong, '*Maximum power tracking for photovoltaic power systems*', Tamkang Journal of Science and Engineering, Vol. 8, N°2, pp. 147 - 153, 2005.

[24] A. Jubaer and S. Zainal, '*An improved perturb and observe (P&O) maximum power point tracking (MPPT) algorithm for higher efficiency*', Applied Energy, Vol. 150, C, pp. pp. 97 - 108, 2015.

[25] N. Kasa, T. Iida and L. Chen, '*Flyback inverter controlled by sensorless current MPPT for photovoltaic power system*', IEEE Transactions on Industrial Electronics, Vol. 52, N°4, pp. 1145 – 1152, 2005.

[26] A.W. Leedy and K.E. Garcia, '*Approximation of P–V characteristic curves for use in maximum power point tracking algorithms*'. In: Proceedings of the system theory (SSST) 45th south eastern symposium. pp. 93 - 88, 2013.

[27] A. Menadi, S. Abdeddaim, A. Betka and M. Benchouia, '*Real Time Implementation of A Fuzzy Logic Based Mppt Controller for Grid Connected Photovoltaic System*', International Journal of Renewable Energy Research, Vol. 5, N°1, pp. 236 - 244, 2015.

[28] H. Sahraoui, L. Chrifi-Alaoui, S. Drid and P. Bussy, '*Second Order Sliding Mode Control of DC-DC converter used in the Photovoltaic System according an Adaptive MPPT*',. International Journal of Renewable Energy Research, Vol. 6, N°2, pp. 375 - 383, 2016.

[29] A. Sarigiannidis, S. Stathis and A. Kladas, '*Performance evaluation of MPPT techniques for PV array incorporated into Electric Vehicle roof*', 4th International Conference on Renewable Energy Research and Applications (ICRERA), Palermo, Italy, 22-25 Nov 2015, pp. 1069 - 1073, 2015.

[30] Y. Soufi, M. Bechouat, S. Kahla and K. Bouallegue, '*Maximum power point tracking using fuzzy logic control for photovoltaic system*', 3rd International Conference on Renewable Energy Research and Applications (ICRERA), Milwakuee, USA 19-22 Oct 2014, pp. 902 - 906, 2014.

[31] T. Tafticht, K. Agbossou, M.L. Doumbia and A. Cheriti, '*An improved maximum power point tracking method for photovoltaic systems*', Renewable Energy Vol. 33, N°7, pp. 1508 - 1516, 2008.

[32] K. Tey and S. Mekhilef, '*Modified incremental conductance MPPT algorithm to mitigate inaccurate responses under fast-changing solar irradiation level*', Solar Energy, Vol. 101, pp. 333 - 342, 2014.

[33] Y. Zhu, M. Cheng and Q. Wang, '*SM-MRAS Based Sensorless MPPT Control for Dual Power Flow Wind Energy Conversion System*', 4th International Conference on Renewable Energy Research and Applications (ICRERA), Palermo, Italy, 22-25 Nov 2015, pp. 296 - 304, 2015.